



Influence of laser shock peening on irradiation defects in austenitic stainless steels



Qiaofeng Lu^a, Qing Su^b, Fei Wang^a, Chenfei Zhang^c, Yongfeng Lu^c, Michael Nastasi^{a, b, d}, Bai Cui^{a, d, *}

^a Department of Mechanical & Materials Engineering, University of Nebraska–Lincoln, Lincoln, NE 68588, USA

^b Nebraska Center for Energy Sciences Research, University of Nebraska–Lincoln, Lincoln, NE 68588, USA

^c Department of Electrical Engineering, University of Nebraska–Lincoln, Lincoln, NE 68588, USA

^d Nebraska Center for Materials and Nanoscience, University of Nebraska–Lincoln, Lincoln, NE 68588, USA

HIGHLIGHTS

- Laser shock peening generates a dislocation network, stacking faults and deformation twins in stainless steels.
- Dislocations and incoherent twin boundaries serve as effective sinks for the annihilation of irradiation defects.
- Incoherent twin boundaries remain as stable and effective defect sinks at 300 °C.

ARTICLE INFO

Article history:

Received 25 July 2016

Received in revised form

16 March 2017

Accepted 29 March 2017

Available online 31 March 2017

Keywords:

Laser shock peening

Irradiation

In-situ TEM

Stainless steel

Microstructure

ABSTRACT

The laser shock peening process can generate a dislocation network, stacking faults, and deformation twins in the near surface of austenitic stainless steels by the interaction of laser-driven shock waves with metals. In-situ transmission electron microscopy (TEM) irradiation studies suggest that these dislocations and incoherent twin boundaries can serve as effective sinks for the annihilation of irradiation defects. As a result, the irradiation resistance is improved as the density of irradiation defects in laser-peened stainless steels is much lower than that in untreated steels. After heating to 300 °C, a portion of the dislocations and stacking faults are annealed out while the deformation twins remain stable, which still provides improved irradiation resistance. These findings have important implications on the role of laser shock peening on the lifetime extension of austenitic stainless steel components in nuclear reactor environments.

© 2017 Elsevier B.V. All rights reserved.

1. Introduction

With a combination of high ductility, strength, and toughness, austenitic stainless steels are widely used in pipelines and steam generators in light water reactors (LWR). However, two vital problems limit the lifetime of austenitic stainless steel structural components in reactor environments, namely, irradiation damage and stress corrosion cracking (SCC) [1–3]. Irradiation of metals with energetic particles, such as neutrons and heavy ions, results in the formation of vacancy- and interstitial-type point defects [4–6]. The accumulation of these point defects could further evolve into defect

clusters, such as dislocation loops [7,8], stacking fault tetrahedra [9], and voids [10] in stainless steels, depending on the irradiation conditions, including the dose level and temperature. These irradiation defects cause significant structural instability and degradation of mechanical properties of stainless steels in the irradiation environment.

The irradiation tolerance of materials can be improved by microstructural modification via introduction of a high density of defect sinks, such as dislocations [11], grain boundaries [12,13], and nanoscale interfaces [14]. It is expected that the irradiation defect clusters will migrate to and be annihilated at these sinks. For example, nanocrystalline metals of tungsten (W), nickel (Ni), and 304L stainless steels exhibit a higher radiation tolerance than their bulk counterparts due to an increased density of grain boundaries [15–17]. Multilayer nanocomposites with immiscible interfaces,

* Corresponding author. Department of Mechanical & Materials Engineering, University of Nebraska–Lincoln, Lincoln, NE 68588, USA.

E-mail address: bcui3@unl.edu (B. Cui).

such as iron/silicon oxycarbide (Fe/SiOC), copper/niobium (Cu/Nb), and vanadium/silver (V/Ag), can effectively mitigate radiation-induced swelling and a loss of mechanical integrity [18–21]. Oxide-dispersion-strengthened (ODS) stainless steels, which have a dispersion of incoherent particle/matrix interfaces, exhibit an enhanced resistance to void swelling and helium bubble embrittlement [22–25].

Laser shock peening (LSP) is a novel surface modification approach that can mitigate most types of failures of metallic materials, such as fatigue, wear, and SCC [26,27]. In the LSP process, a laser beam hits the sacrificial coating on the surface of the metal target and forms a plasma, which rapidly expands and generates shock waves into the bulk (Fig. 1). The laser-driven shock waves cause significant compressive residual stresses (typically 0.1–1 GPa) that can extend to a depth of more than 1 mm from the surface [28,29]. Compared to traditional mechanical shot peening, LSP offers many advantages, such as deeper penetration of compressive stresses (typically > 1 mm, which is about ten times that of mechanical shot peening), shorter process times (typically several tens of nanoseconds), precise control, accuracy, and flexibility [30,31]. For example, LSP has succeeded in improving the fatigue life of metal components of aircraft structures and engines by General Electric Infrastructure-Aviation and LSP Technologies [32,33]. Recently, there have been a few successful studies that employ LSP to prevent SCC of austenitic stainless steels [34–36]. The improvement of SCC resistance by LSP has been generally attributed to the effect of compressive residual stresses and microstructural changes, although the exact mechanistic mechanism has not been well elucidated [35].

Experimental investigations have revealed that the benefit of LSP is related to the microstructural evolution near the surface of materials during the LSP process. The interaction of laser-driven shock waves with metallic materials causes severe plastic deformation, which can manifest as dislocation networks, deformation twins, and grain refinement [37–39]. Highly tangled and dense dislocations and dislocation-cell structures are observed in aluminum alloys subjected to LSP [38,40]. Grain refinement is observed in 304 stainless steels with the grain size increasing with depth, the mechanism of which is suggested to be caused by twin-twin intersections, which transform to subgrain boundaries [35,37,41]. To our knowledge, no previous research studied the effects of LSP on the irradiation resistance of materials. However, we hypothesize that the modified microstructure on the surface of austenitic stainless steels will change their response to the irradiation damage.

The objective of the research documented by this paper is to determine if LSP can improve the irradiation resistance of austenitic stainless steels. The microstructural evolution of austenitic stainless steels during the LSP process was studied using transmission

electron microscopy (TEM). The irradiation behavior of laser-peened austenitic stainless steels was investigated using in-situ TEM irradiation experiments at the intermediate voltage electron microscope (IVEM)-Tandem facility at the Argonne National Laboratory to directly observe the dynamics of interactions of irradiation defects with potential sinks, such as dislocations and twin boundaries. The thermal stability of as-formed microstructures was also observed by in-situ TEM heating experiments from room temperature to 300 °C, which is around the operating temperature of LWR. These findings have important implications on the lifetime extension of austenitic stainless steel components in nuclear reactors by LSP. That is, in addition to its well-known effect of preventing fatigue and SCC, LSP may also improve the irradiation resistance of austenitic stainless steels.

2. Material and methods

Commercial purity 304 stainless steels (Fe-18.3% Cr-8.5% Ni-1.38% Mn-0.65% Si-0.03% S-0.04% C by weight) were used as model materials in this study. The static yield strength is 290 MPa. The sample was annealed at 950 °C for 30 min under Ar atmosphere. The initial microstructural characterization showed a grain size of 25–50 μm, a low dislocation density and no precipitates.

In the LSP experiments, the geometrical dimensions of samples were 10 mm × 8 mm × 2 mm, which were cut using a diamond saw. The samples were ground using silicon carbide (SiC) grinding papers, followed by polishing using 3 μm and 0.3 μm alumina powders. LSP was performed using a Q-switched Nd:YAG laser source at room temperature. Typical parameters of the LSP process, such as the laser pulse energy, laser pulse number, spot diameter, pulse duration, and overlap ratio are listed in Table 1. The magnitude and depth of compressive residual stress generated by LSP is increased with the laser energy and the number of LSP scans [36,42]. Therefore, the highest laser energy in the Nd:YAG laser (850 mJ) was chosen in this study and the sample was treated by LSP for 5 times. Scanning the laser beam can enable LSP on an area of 10 mm × 8 mm of the 304 stainless steel samples. The sample surface was coated with a 177 μm thick black tape as a sacrificial layer to avoid laser ablation. A flowing film of deionized water covered the sample surface, which acted as the plasma-confining media [27,34]. It is important to note that in this LSP process, the metal samples remained at room temperature with the protection of the sacrificial layer and the water film.

3. Experimental

The near-surface microstructure of 304 stainless steels was characterized by transmission electron microscopy (TEM) after the LSP process. The specimens were cut from the region close to the surface and thinned to a thickness of less than 100 μm by mechanical polishing. Final thinning to electron transparency was performed using a twin jet polisher with a 5% perchloric acid and 95% methanol electrolyte at –20 °C. Assuming the electropolishing

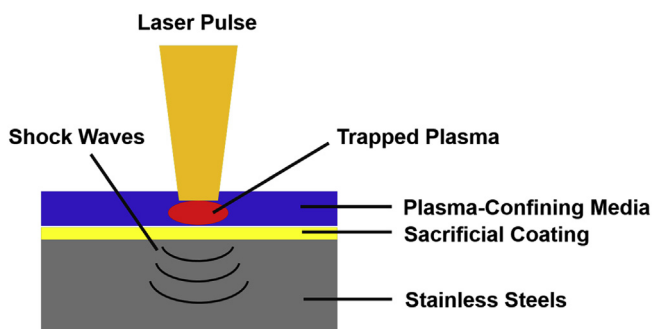


Fig. 1. Schematic of the LSP process of stainless steels.

Table 1

Typical experimental parameters for LSP of austenitic stainless steels.

Pulse energy (mJ)	850
Spot diameter (mm)	1
Pulse duration (ns)	7
Number of LSP scans	5
Overlap ratio	50%
Repetition-rate (Hz)	10
Laser wavelength (nm)	1064
Beam profile	Gaussian

Download English Version:

<https://daneshyari.com/en/article/5454346>

Download Persian Version:

<https://daneshyari.com/article/5454346>

[Daneshyari.com](https://daneshyari.com)